# A method for determination of tracheobronchial airway geometries from four different strains of mice

PMI SCIENCE
PHILIP MORRIS INTERNATIONAL

C. Foong[b], M.J. Oldham[c], F. Lucci[a], S. Cockram[d], S. Luke[d], D. Yeo[b], J. Chua[b], J. Hoeng[a], M. Peitsch[a], A.K. Kuczaj[a,*]

[a] PMI R&D, Philip Morris Products S.A., Neuchâtel, Switzerland
[b] PMI Research Laboratories Pte. Ltd., Singapore
[c] Former Altria Client Services LLC employee, Richmond, USA
[d] Synopsys, Exeter, United Kingdom

* Corresponding author: arkadiusz.kuczaj@pmi.com

## Introduction

Accurate lung morphometry is one of the key elements in estimating the delivered aerosol dose from animal exposure studies and is crucial for biological dose response analyses (Figure 1).

Currently, lung morphometry is only available for three strains of mice (B6C3F1, BALB/c, and A/J). Utilizing *in situ*-prepared silicone rubber mouse lung casts, a complete process, including micro-CT scanning, segmentation, and automated algorithmic processing enabling determination of airway geometries, was developed and used on three strains of mice (BALB/c, ApoE$^{-/-}$, and C57BL/6).

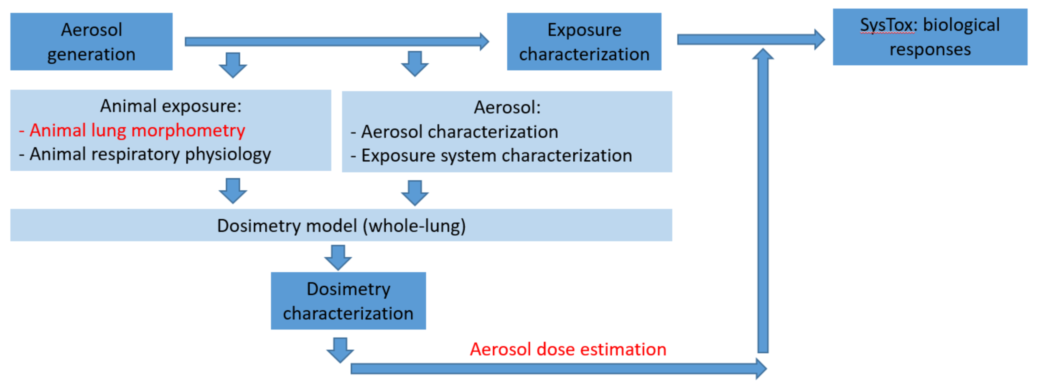


**Figure 1.** Aerosol exposure and dosimetry. Schematic workflow (top) including the animal lung morphometry steps (bottom).

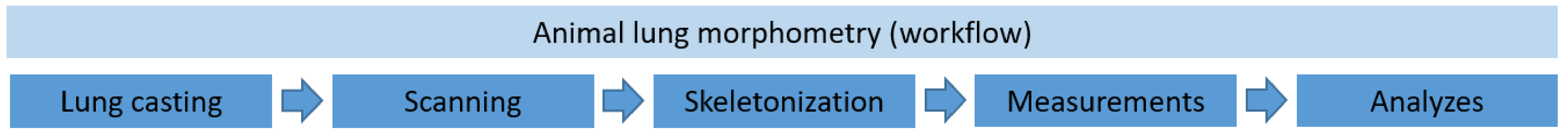


## Lung casting preparation and scanning

Brief recent history of *in situ* lung casting:
- 1973: Refined *in situ* technique by Phalen et al. in rats
- 1978: Further refined by Phalen et al. in rats
- 1994: First used in B6C3F1 mice by Oldham et al.
- 2002: Used in BALB/c mice by Oldham & Phalen

Silicone rubber lung casts were prepared *in situ* from ApoE$^{-/-}$ and C57BL/6. Further *in situ* casts were already available from BALB/c mice (Islam et al., 2017) and A/J mice. The cured mouse lung casts were manually inspected for casting quality, and manual morphometry measurements were performed (tracheobronchial generations 1–6) on selected lung casts prior to high-resolution micro-CT scanning. The casts were scanned with a commercially available cone-beam micro-CT (µCT 100, SCANCO Medical AG, Switzerland) that allowed voxel resolution of 6.6 µm.

Tracheobronchial tree (Figure 2: idealized view for measurements, Figure 3: typical cast example)

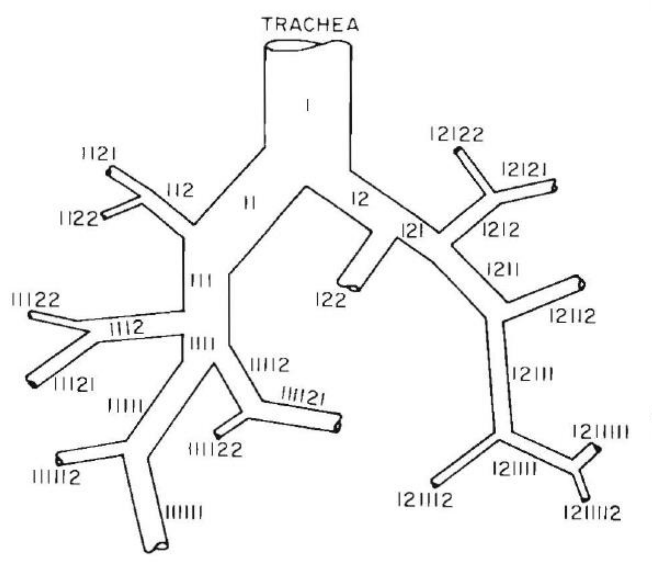


**Figure 2.** Idealized model defining parameters for morphometric measurements. Source: Phalen RF, Oldham MJ, Tracheobronchial airway structure as revealed by casting techniques, Am. Rev. Respir. Dis., 1983, 128: S1-S4.

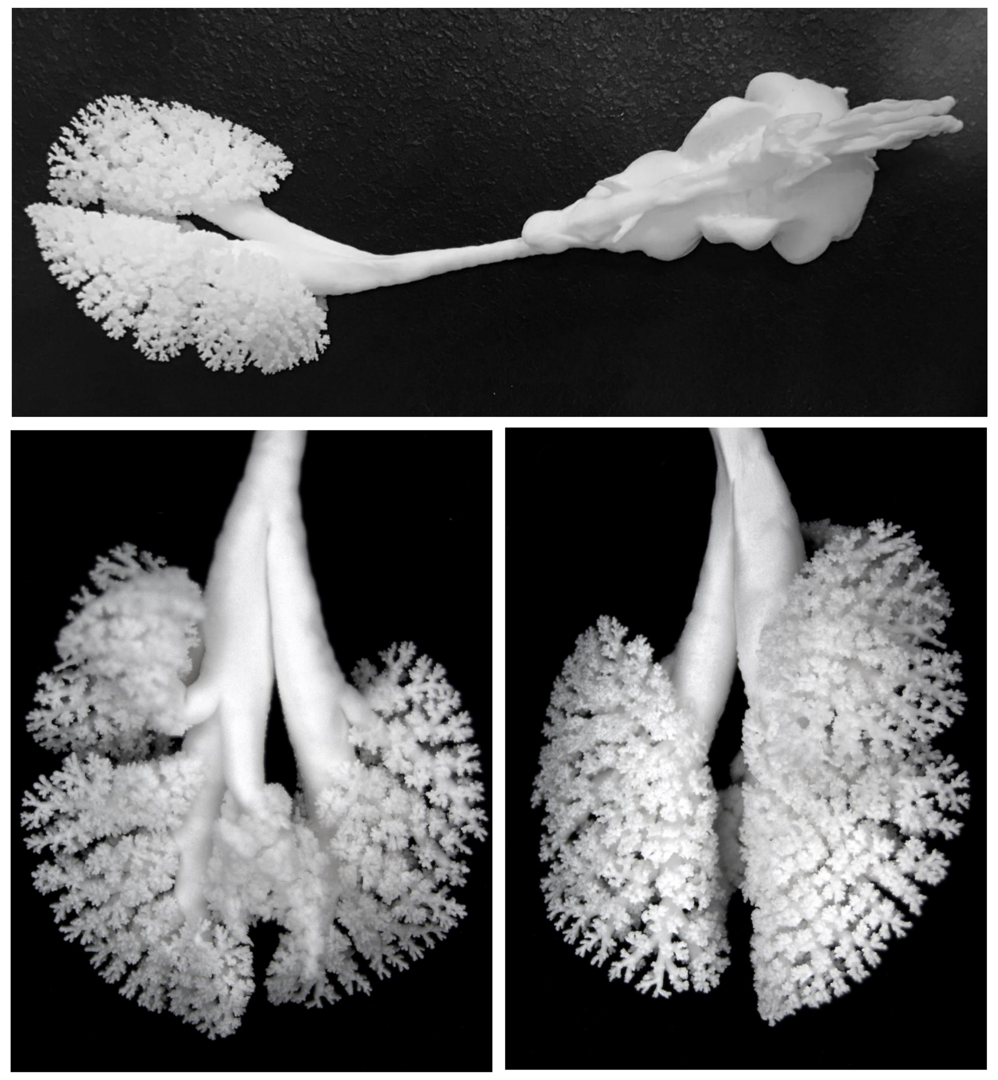

Measurements were performed including:
- Number of airways (branch count)
- Airway length (mm)
- Airway diameter (mm)
- Bifurcation angle (°)
- Inclination to gravity angle (°)

**Figure 3.** Example of the analyzed cast (Cast 10). Left: full, front, and back views; below: characteristics).

| Strain | ApoE$^{-/-}$ |
|---|---|
| Gender | Female |
| Age at time of casting (weeks) | 18-20 |
| Bodyweight at time of casting (g) | 25.5 |
| Length (cm) | 10.3 |

## Skeletonization and measurements

The micro-CT images from 11 of the prepared casts were segmented to reconstruct 3D models of individual lung casts using Synopsys Simpleware ScanIP software (Young et al., 2008). A skeleton of each processed lung cast was automatically created by shrinking the 3D model of each airway to its centerline (Figure 4).

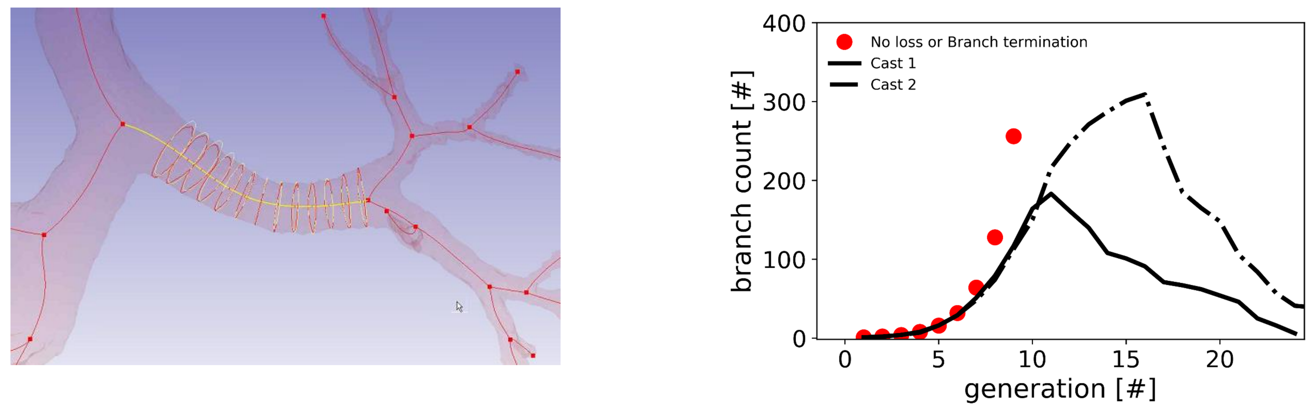


**Figure 4.** Developed method for automated computation of tracheobronchial tree characteristics.

Algorithms were developed for automatic detection of possible skeleton exceptions, such as closed loops, trifurcations, and isolated nodes, to be subsequently resolved manually. Finally, the skeleton was automatically measured, extracting major airway morphometry characteristics (see examples of data processing in Figure 5).

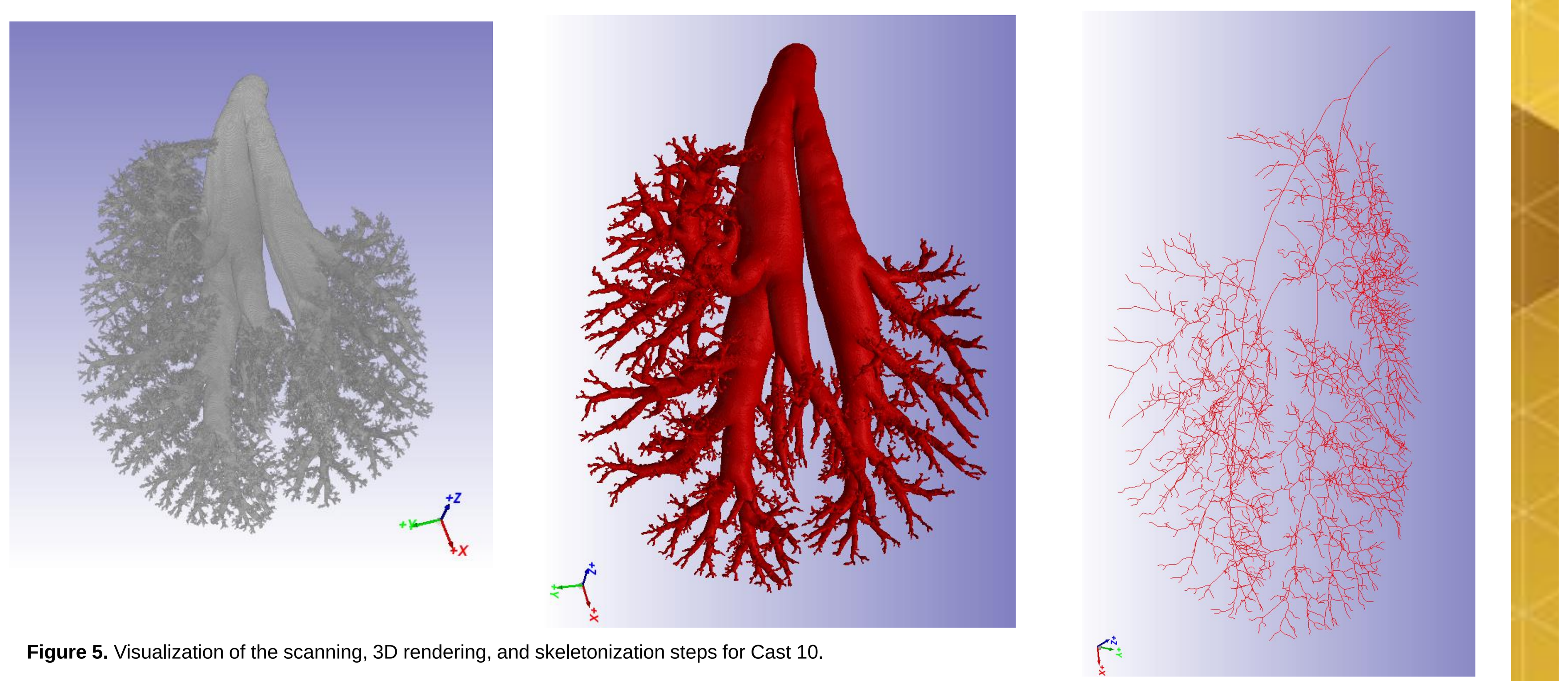

**Figure 5.** Visualization of the scanning, 3D rendering, and skeletonization steps for Cast 10.

The automated measurement procedure was tested/verified by comparing its measurements of airway length, diameter, and bifurcation angle with previous measurements (Islam et al., 2017). Comparison was performed against both manual morphometry measurements and the automated measurements of lung casts of two BALB/c mice (Figure 6). A reasonable agreement between all the measurement procedures was observed for the length and the diameter. More discrepancies were observed in the measurements of the bifurcation angles, which are attributed to the difficulties in measuring the angles due to the short length of the airways (Islam et al., 2017).

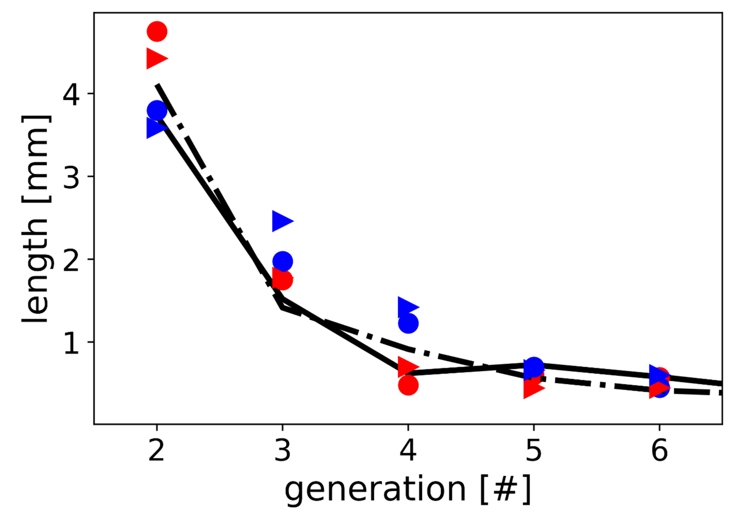


**Figure 6.** Validation performed on the obtained geometries of Cast 1 and Cast 2 from Islam et al. Left: length of branches versus lung generation number; bottom left: diameter of branches; bottom right: bifurcation angle.

Cast 1: current method
Cast 1: Islam et al. – manual
Cast 1: Islam et al. – automated
Cast 2: current method
Cast 2: Islam et al. – manual
Cast 2: Islam et al. – automated

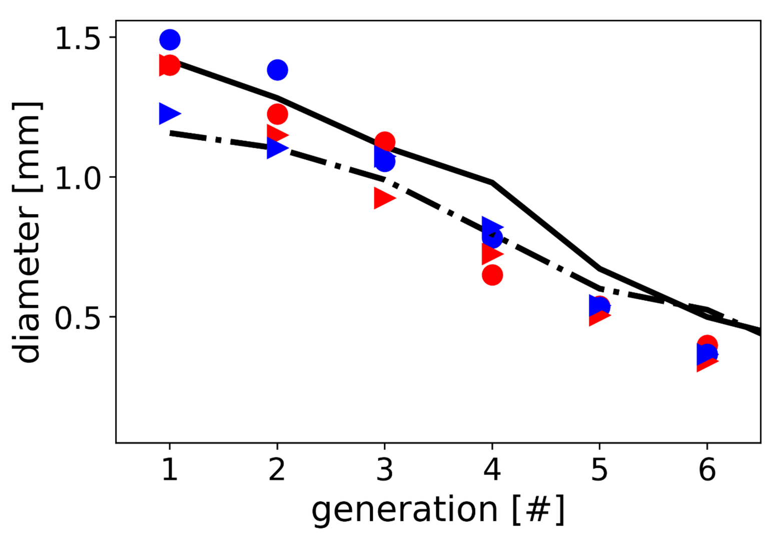


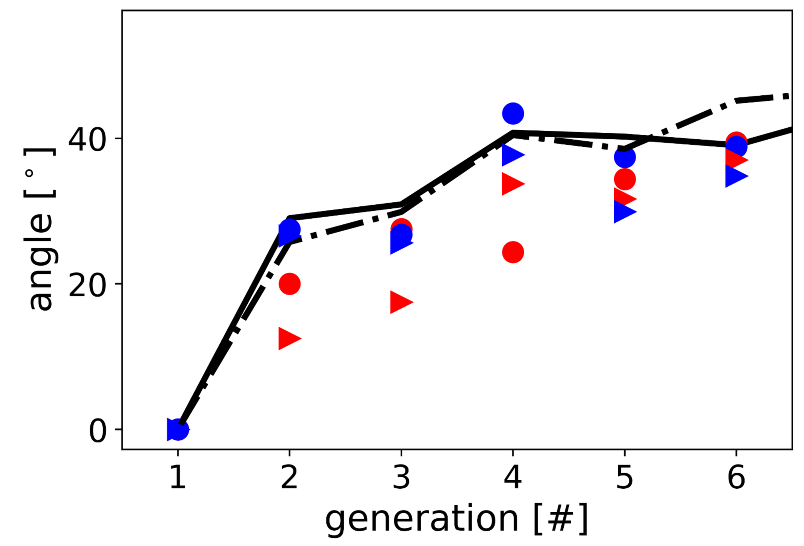


## Analysis

With the described procedure, a skeleton with more than 2,000 branches was generated for each lung cast. With the current resolution, some branch data was collected approximately down to generation 25. However, the analysis of the branch count statistics (Figure 4) suggests that at present, the data analysis can be considered of significance only down to generations 9-10, where the majority of the branches have been captured and analyzed. In Figure 7, airway length, diameter, and bifurcation angle statistics are shown for the segmented lung casts. Tracheobronchial airway lengths and diameters show similar values between both strains, especially when the differences in body weight are considered. While tracheobronchial airway diameters for ApoE$^{-/-}$ and C57BL/6 mice were similar, they were significantly different from the BALB/c mice examined. The latter presents approximately 50% smaller tracheobronchial airway diameters, which is expected to have an influence on the aerosol deposition.

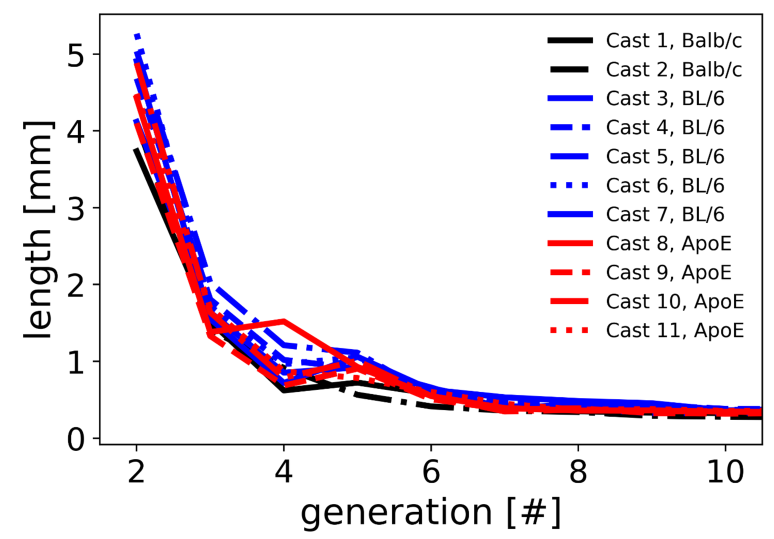


**Figure 7.** Measurements performed for airway length, airway diameter, and bifurcation angle versus airway generation number for the casts of BALB/c, C57BL/6, and ApoE$^{-/-}$ mice characterized in the table.

| Name | strain | age(wks) | bodyweight(g) | length(cm) |
|---|---|---|---|---|
| Cast 1 | Balb/c | - | 24.4 | - |
| Cast 2 | Balb/c | - | 25.9 | - |
| Cast 3 | BL/6 | 12-14 | 24.4 | 9.3 |
| Cast 4 | BL/6 | 13-15 | 27.5 | 9.8 |
| Cast 5 | BL/6 | 15-17 | 30.6 | 9.7 |
| Cast 6 | BL/6 | 16-18 | 23.8 | 10.1 |
| Cast 7 | BL/6 | 16-18 | 21.7 | 9.1 |
| Cast 8 | ApoE | 18-20 | 25 | 10.2 |
| Cast 9 | ApoE | 18-20 | 23.4 | 9.8 |
| Cast 10 | ApoE | 18-20 | 25.5 | 10.3 |
| Cast 11 | ApoE | 40-42 | 23.6 | 10 |

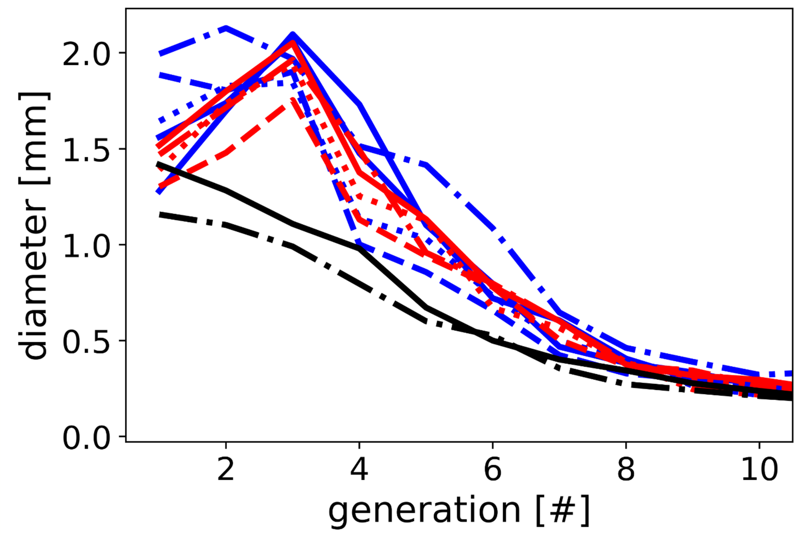


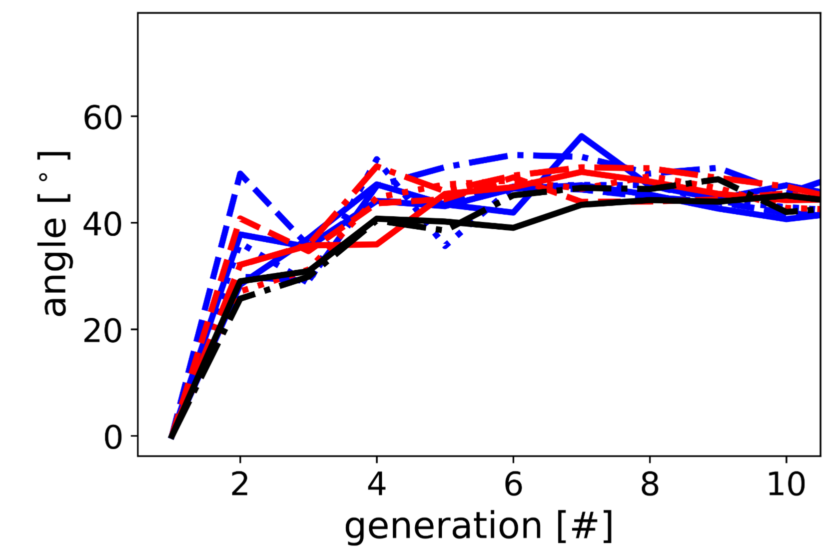


## Summary

- A set of 20 silicone rubber lung casts was obtained from ApoE$^{-/-}$, C57BL/6, BALB/c, and A/J mice.
- Automated algorithms were developed and applied in measurements of major airway morphometry characteristics (e.g., airway generation count, length, diameter, bifurcations angles, and angle to gravity) for 11 of the available lung casts.
- Tracheobronchial airway diameters for ApoE$^{-/-}$ and C57BL/6 mice were similar but were significantly different from the BALB/c murine strains examined.
- Further analyses are ongoing on ApoE$^{-/-}$ and A/J casts to complete the measurements and analyses with the ultimate goal of delivering data for aerosol deposition models (NCRP, ICRP, and Multiple-Path Particle Dosimetry Model).

## Literature

- Phalen et al. Casting Lungs in-Situ. Anat Rec. 1973;177(2):255–63.
- Oldham et al., Predicted Nasal and Tracheobronchial Particle Deposition Efficiencies for the Mouse. Ann. Occup. Hyg. 1994, 38 (Supp. 1):135–141.
- Oldham, M. J. and Phalen, R. F., Dosimetry Implications of Upper Tracheobronchial Airway Anatomy in Two Mouse Varieties. Anat. Rec. 2002, 268:59–68.
- Islam A., Oldham M.J., Wexler A.S., Comparison of Manual and Automated Measurements of Tracheobronchial Airway Geometry in Three Balb/c Mice, Anat. Rec., 2017, 300(11):2046-2057
- Young P.G., Beresford-West T.B., Coward S.R., Notarberardino B., Walker B., Abdul-Aziz A., An efficient approach to converting three-dimensional image data into highly accurate computational models, Philos Trans A Math Phys Eng Sci., 2008, 366(1878):3155-3173

SOT Baltimore 2019

**Competing Financial Interest** – The research described in this poster was sponsored by Philip Morris International